Miscible Blends of Cellulose and Poly(vinylpyrrolidone)

Jean-François Masson† and R. St. John Manley*

Pulp and Paper Research Centre and Department of Chemistry, McGill University, 3420 University Street, Montreal, Quebec, Canada H3A 2A7

Received January 29, 1991; Revised Manuscript Received July 22, 1991

ABSTRACT: Cellulose was dissolved in the solvent system dimethyl sulfoxide–paraformaldehyde (DMSO–PF) and blended with poly(vinylpyrrolidone) (PVP) dissolved in DMSO. The homopolymers and blend films were solution cast at 25 °C under reduced pressure. To ascertain the state of miscibility of the blends, they were investigated by using wide-angle X-ray scattering (WAXS), Fourier transform infrared (FTIR) spectroscopy, differential scanning calorimetry (DSC), dynamic mechanical analysis (DMA), and solid-state magic-angle spinning (CP-MAS) NMR. X-ray analysis revealed that in the blends each polymer influences the structural order of the other. A detailed estimation of the glass transition temperature (T_g) by DMA revealed that cast cellulose displays a T_g at 208 °C and that every blend shows a single T_g, which varies with composition. The increase in T_g in going from the T_g of PVP to the T_g of cellulose is not monotonic but shows a discontinuity at a composition of ca. 60% (w/w) cellulose. This behavior is tentatively interpreted in relation to the molar ratio of the repeating units of the constituent polymers. The miscibility was shown, from FTIR and CP-MAS NMR, to be driven by the interaction between a portion of the ensemble of the carbonyl groups of PVP and the primary hydroxyl functionalities of cellulose. From solid-state CP-MAS NMR measurements of proton $T_{1\rho}$ relaxation times, it is suggested that below the discontinuity in the T_g vs composition curve the two polymers mix on a scale of ca. 2.7 nm and that above the discontinuity they mix on a scale between 2.7 and 15 nm.

Introduction

During the past decade, intense interest has been focused on polymer blends in which both components are synthetic polymers.[1,2] In contrast, few studies[3-9] have been made on blends in which one component is cellulose. Nevertheless, cellulose/synthetic polymer blends are attractive and important not only because of potential applications but more especially as models for the investigation of blends containing polymers with functional groups that can engage in strong intermolecular interaction such as hydrogen bonding.

For thermodynamic miscibility in polymer blends a basic prerequisite is that the Gibbs free energy of mixing be negative. For this purpose it is usually necessary to have some kind of favorable interaction between segments of the component polymer chains. Because of the abundance of hydroxyl groups in cellulose, blends with synthetic polymers offer the interesting possibility of studying the effects of strong hydrogen bonding as a major factor in inducing miscibility. Thus for blending with cellulose it is important to choose synthetic polymers containing functional groups that can potentially interact with the hydroxyl groups of the cellulose chains. Many important synthetic polymers fall into this category, notably, polyamides, polyesters, and vinyl polymers such as poly(vinyl alcohol) and polyacrylonitrile. Thus in recent studies it has been shown that cellulose/poly(vinyl alcohol),[4] cellulose/polyacrylonitrile,[3] and cellulose/poly(ethylene oxide)[7] are miscible pairs.

In the present work we have extended the study of cellulose/synthetic polymer blends to the system cellulose/poly(vinylpyrrolidone). The latter has been chosen not only because it is amorphous and does not self-associate but also because the interactions between the carbonyl and the cellulose hydroxyl groups are expected to favor miscibility.

Blends covering the entire composition range were prepared by casting from mixed polymer solutions in dimethyl sulfoxide. We characterized the phase behavior of the blend pair by several methods. The state of miscibility was quantified by measuring the T_g by means of thermal analysis and dynamic mechanical testing.[1,2,10] From X-ray analysis, we monitored the changes in the diffraction patterns of the constituent polymers as we varied the blend composition. With infrared and NMR spectroscopy, we scanned for specific interactions between the polymer moieties. Finally, we estimated the scale of phase separation produced upon blending the two polymers by spin-diffusion measurements.[11-13]

Experimental Section

Materials. The cellulose sample used was a dissolving pulp (Temalfa A) kindly supplied by Tembec (Temiscamingue, Quebec, Canada); the degree of polymerization was 870. The other polymer, poly(vinylpyrrolidone) purchased from Aldrich Chemical Co. (cat. no. 85,647-9), was dried at 100–105 °C and kept in a desiccator over calcium chloride until used; the nominal molecular weight was 360 000. Dimethyl sulfoxide (HPLC grade, cat. no. 27,043-1) and paraformaldehyde (cat. no. 15,812-7), both purchased from Aldrich Chemical Co., were used as supplied.

Preparation of Samples. The dissolution of cellulose was carried out in a manner analogous to the procedure described by Seymour and Johnson.[14] Cellulose (5 g) was stirred in the presence of paraformaldehyde (PF) (9.6 g) in dimethyl sulfoxide (DMSO) (260 g) at 65–70 °C. After 20 h of heating, a clear and viscous solution resulted. The viscosity of this solution was reduced by the addition of ca. 100 mL of solvent. The excess PF present in solution was removed by leaving the solution under vacuum until bubbling of the solution ceased. The complete removal of residual PF was attested when no bubbles were produced when an aliquot of the solution was heated at 130 °C, a temperature at which PF decomposes violently to produce formaldehyde. The concentration of the cellulose solution was calculated to be 1.37%. A 3.20% solution of poly(vinylpyrrolidone) (PVP) was prepared in a few hours by stirring the polymer in DMSO at room temperature.

The two solutions thus separately prepared were mixed in appropriate amounts to give blends of various compositions ranging from 10/90 to 90/10 in ratio of weight percent, the first numeral referring to cellulose throughout this paper. After the blend solutions were stirred for at least 2 days at room temperature, the blend films were obtained by slow casting under reduced

* To whom correspondence should be addressed.
† Present address: National Research Council of Canada, Institute for Research in Construction, Ottawa, ON, Canada K1A 0R6.

0024-9297/91/2224-6670$02.50/0

pressure in polypropylene dishes over a period of 4 days. Once casting was complete, the films were kept at 75 °C in vacuo for an additional 4 days. Finally, to remove as much residual DMSO as possible, each film was kept at 195 °C for 5 min in a nitrogen atmosphere, unless otherwise stated. All samples were kept in a desiccator over calcium chloride until measurements were performed.

Measurements. Wide-angle X-ray scattering (WAXS) patterns of the different blends were recorded with a flat-film camera with the use of nickel-filtered Cu Kα radiation produced by a Philips X-ray generator operating at 40 kV and 20 mA.

Density measurements were made at 23 °C with a density gradient column containing carbon tetrachloride and xylene and calibrated between 1.10 and 1.55 g/cm³. The reported sample densities are the averages of three measurements.

The molar substitution (MS) of the anhydroglucose unit was determined from the amount of formaldehyde liberated upon immersion of methylolcellulose in an aqueous solution of sodium sulfite. The formaldehyde, produced by hydrolysis of the methylol groups, reacts with sodium sulfite to produce sodium hydroxide.[15] From the acid titration of the latter and the weight of the cellulose recuperated, the MS was readily calculated. The amount of DMSO present in the film was estimated from the total weight lost upon immersion. Typically 500 mg of cast film was steeped in a 0.5 M solution of sodium sulfite, and after waiting 24 h to ensure complete hydrolysis of the methylol groups, the basic mixture was titrated with 0.05 M hydrochloric acid.

Differential scanning calorimetry (DSC) was performed in a Perkin-Elmer Model DSC-7 instrument operated with the TAS-7 data station on the samples (12–15 mg) after they had been dried for 4 days at 75 °C. The instrument was calibrated with an indium standard and operated at a heating rate of 20 °C/min. The samples were thermally analyzed in a nitrogen atmosphere in two scans between 100 and 240 °C. The first scan showed a broad endotherm between 150 and 200 °C due to the presence of residual water and/or solvent. The second scan showed no such endotherm. Between the two heating scans the samples were kept at 240 °C for 3 min and then quenched to 100 °C. The reported glass transition temperatures are those from the second heating scan.

Fourier transform infrared (FTIR) spectroscopy of the blend films was performed on a Mattson Instrument Inc. Model Cygnus 25 photoacoustic FTIR spectrometer. The resolution was 8 cm^{-1} and 100 signal-averaged scans were performed and stored on a magnetic disk. Infrared spectra of the PVP solutions were acquired on an Analect RAM-56 FTIR spectrometer operated with a MAP-67 control station. A minimum of 64 scans were signal-averaged at a resolution of 2 cm^{-1}. The frequency scale was internally calibrated with a reference helium-neon laser to an accuracy of 0.2 cm^{-1}. The concentration of the PVP solutions was approximately 2% by weight.

The dynamic storage modulus E', loss modulus E'', and mechanical loss tangent tan δ of cellulose and blend films were measured with a Rheovibron Model DDV-II viscoelastometer (Toyo Baldwin Co., Ltd.) at 11 Hz in a nitrogen atmosphere. The samples cut from the cast films had typical dimensions of 2.0 × 0.5 × 0.005 cm. PVP was run on a dynamic mechanical thermal analyzer (DMTA) (Polymer Laboratories Inc.) at 10 Hz. In this case the sample had a free length, a width, and a thickness of 1.6, 1.2, and 0.2 cm, respectively. In the runs on both the Rheovibron and the DMTA the temperature was raised at a rate of 1.5 ± 0.2 °C/min in the range 30–220 °C.

All solid-state NMR experiments were performed with a dedicated solid-state Chemagnetics Inc. M-100 spectrometer equipped with a magic angle spinning probe. The blend films cut in squares of ca. 1 mm^2 were packed in zirconia rotors equipped with Kel-F end caps. Spinning rates were generally 3.5–4.0 kHz. A 90° pulse width of 5 μs was employed with 5000–10 000 fid signal accumulations depending on the amount of sample and composition of the blend. The Hartmann–Hahn match was adjusted prior to every run with hexamethylbenzene. Chemical shifts were referred to tetramethylsilane using the methyl carbon of hexamethylbenzene at 17.45 ppm. Proton spin–lattice relaxation times in the rotating frame were measured via carbon signal intensities using a ^1H spin–lock–τ sequence prior to cross polarization.[16] Acquisition was performed with ^1H decoupling, and delay times (τ) ranged from 1 to 10 ms. All spectra were obtained at room temperature.

Table I
Molar Substitution of Cellulose and Dimethyl Sulfoxide Content as a Function of Temperature

	temp, °C			
	25[a]	75[a]	140[b]	195[b]
molar substitution	2.38	1.98	1.60	0.78
DMSO per AHG[c] unit, mol/mol	0.78	0.36	0.28	0.28

[a] Four days in vacuo. [b] Five minutes in a nitrogen atmosphere. [c] AHG: anhydroglucose.

Results and Discussion

Cast Cellulose. It is well-known[14,17–21] that the dissolution of cellulose in the system DMSO–PF proceeds via the formation of methyolcellulose, a hemiacetal derivative. The molar substitution (MS) of the anhydroglucose unit depends on the temperature at which the cellulose is dissolved.[17,19,20] When the temperature of dissolution is 125–130 °C, the MS varies between 1.0 and 6.1.[17,19,22] The use of a lower dissolution temperature, like that used in this study, has been shown to produce a product with a MS as high as 18.8;[20] under these conditions each of the three hydroxyl groups of cellulose is substituted with a poly(oxymethylene) chain.[20] The recuperation of essentially undegraded and unsubstituted cellulose can be achieved by hydrolysis of the methylol adduct with the addition of water or a protic solvent.

Upon mixing cellulose and PVP, however, the blend must be recuperated by some other means than coagulation since PVP will coagulate to form a film only with difficulty once it is in solution. Thus it is necessary to cast the films of cellulose, PVP, and the cellulose/PVP blends to obtain comparable solid samples. Because prolonged heating of the cellulose solution at 85 °C has been shown[20] to decrease the MS and since paraformaldehyde rapidly decomposes to volatile formaldehyde even at moderate temperature, we expected regeneration of unsubstituted cellulose from casting the DMSO solution and heat-treating the resulting film. The data in Table I show that the regeneration process proceeds almost to completion. From an estimated initial value of close to 20, the MS is reduced to 2.38 after the casting period and 4 days in vacuo at 25 °C. It is interesting to note that this film does not redissolve in DMSO, in contrast with samples with a lower MS of 1.1 obtained by freeze-drying.[17] An additional 4 days at 75 °C causes the MS of the solid cellulose film to decrease to 1.98. Further heat treatment at 140 and 195 °C for 5 min causes the MS to decrease to 1.60 and 0.78, respectively. From the data of Table I, we can also note that the effective number of DMSO molecules per anhydroglucose unit of cellulose remains constant at 0.28 after treatment at 140 or 195 °C. Treating the samples for times up to 1 h at 195 °C does not reduce any further the amount of DMSO that remains bound to cellulose. The steeping of the cellulose films in nonprotonated solvents miscible with DMSO but incapable of dissolving PVP, for example, ethyl ether, acetone, or carbon tetrachloride, does not remove DMSO either. Presumably, the complete removal of DMSO is hampered by strong interaction between the hydroxyl groups of cellulose and the sulfoxide group of DMSO.

Visual Observations. The initial cellulose solution was clear at a concentration of ca. 2% in contrast to solutions obtained by Seymour and Johnson,[14] which were opaque at concentrations higher than 0.5% under similar conditions. The PVP solution and all the blend solutions

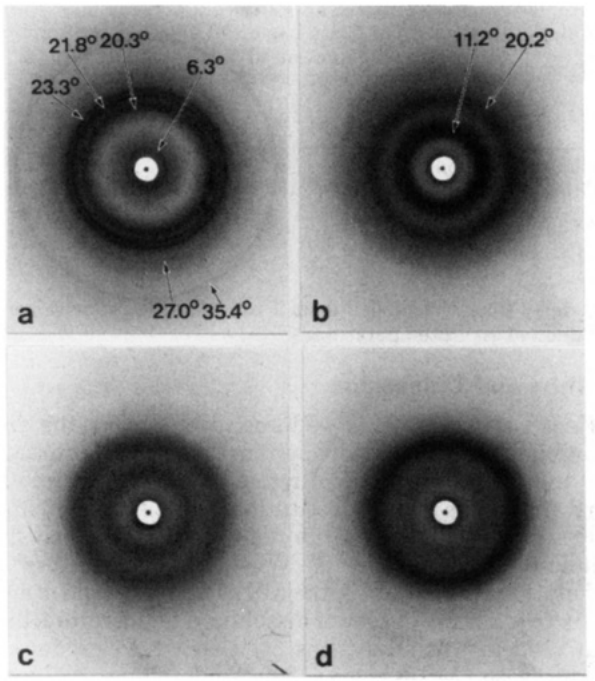

Figure 1. Wide-angle X-ray diffraction patterns for films prepared by casting from DMSO–PF solutions: (a) cellulose; (b) PVP; (c) 20:80 cellulose/PVP; (d) 70:30 cellulose/PVP.

were also clear to the naked eye. The solutions showed neither any phase separation into bilayers nor the appearance of a precipitate even after 8 months at room temperature. Cast films of both homopolymers and their blends were clear irrespective of the blend composition. Viewed under the optical microscope, all the cast samples had a uniform appearance. No phase separation above micron size could be perceived.

WAXS Characterization. The WAXS pattern of the cast cellulose film is shown in Figure 1a, and Table II summarizes the 2θ values of the observed maxima. Such a diffractogram suggests the existence of a cast cellulose crystal lattice different from the known cellulose[23] polymorphs. This crystal lattice presumably owes its existence to the presence of methylol adducts, partially substituting the ensemble of the hydroxyl groups, and the presence of complexing DMSO molecules. Depletion of the methylol substituent from cellulose and removal of the DMSO by steeping the film in hot water for at least 1 h permits rearrangement of the cellulose chains into the more familiar monoclinic unit cell characteristic of cellulose II.

The WAXS pattern of PVP (Figure 1b) shows two halos centered at $2\theta = 11.2$ and 20.2°. The halo at 20.2° corresponds to scattering produced by short-range order in the noncrystalline regions while the more intense maximum at 11.2° arises from a pseudocrystalline phase.[24] The WAXS pattern of the blends shows no evidence of a mixed-crystal structure that could arise from the interaction of the crystalline and pseudocrystalline phases of the respective polymers. However, the diffractograms of the blends are all different from a true superposition of the patterns of the two homopolymers. It is qualitatively observed that by mixing the two polymers the relative intensities of several maxima are significantly reduced. For example, in the WAXS pattern of the 70:30 blend (Figure 1d), the three sharper maxima of cellulose at 20.3, 21.8, and 23.3° can no longer be distinguished from one another but appear as a halo, while the maximum that was centered at 11.2° in pure PVP is almost totally absent. In the 20:80 blend (Figure 1c), this same diffraction at 11.2° no longer has a stronger intensity than the one at 20.2°, which overlaps indistinguishably with the now weak reflections of cellulose at 20.3, 21.8, and 23.3°. Each blend with a cellulose/PVP composition between 20:80 and 80:20 shows a broad diffraction maximum arising from the overlapping maxima produced by the amorphous regions of the respective polymers; no reflections arising from ordered or pseudoordered regions are observed. It thus appears that in the blends each polymer influences the structural order of the other.

FTIR Measurements. Infrared spectra were acquired on the cellulose/PVP blends and on solutions of PVP in various alcohols. The carbonyl band of PVP was examined for changes in line shape and/or frequency which might indicate a specific interaction with cellulose. Shifts to lower frequencies and line broadening can reveal the involvement of the carbonyl groups in hydrogen-bonding type of interactions.[25] Figure 2 shows the carbonyl region of the infrared spectra for pure PVP and two cellulose/PVP blends. Characteristic of pure PVP is a rather broad band centered at 1681 cm^{-1}. When PVP is blended with cellulose, a shoulder on the carbonyl band appears at 1656 cm^{-1} as shown for the 30:70 blend. This shoulder, also observed upon mixing PVP with poly(vinylphenol), has been assigned to hydrogen-bonded carbonyl groups.[26] In the 90:10 blend, both the 1681- and 1656-cm^{-1} bands are clearly present although the carbonyl groups are largely outnumbered by the hydroxyl functionalities. This indicates a partial involvement of the carbonyl functionalities in the interaction with cellulose. In complement, these spectra demonstrate that interactions at the molecular level are present in the blends.

Because stronger interactions manifest larger shifts, a comparison of the shift recorded in the cellulose/PVP blends with the shift produced by dissolving PVP in alcohols might inform us on the relative strength of the hydrogen bonding in which the carbonyl group is involved in the blends. The results are shown in Table III. The dissolution of PVP in a solvent that has a readily accessible hydroxyl group, like methanol or 1,4-butanediol, produces a shift of the carbonyl band frequency of 17 cm^{-1}. Substituting these solvents for cyclohexanol, which has a more sterically hindered hydroxyl group, produces a smaller shift of 12 cm^{-1}. The viscous poly(ethylene glycol)-400, with a much lower degree of freedom than the other solvents used here, lowers the carbonyl band frequency by 5 cm^{-1} in comparison with pure PVP. In contrast, cellulose with its molecular weight of ca. 141 000 and relatively rigid structure interacts more strongly with PVP than any of the other alcohols, since the carbonyl band shows a shift of 25 cm^{-1}. It is thus possible that more than one hydroxyl group of cellulose interacts with the same carbonyl functionality of PVP. In other words, a single carbonyl group can interact simultaneously with several hydroxyl groups, be they from the same or from different anhydroglucose units.

As a consequence of the interaction between the two moieties, we might expect an increase in the density of the blends over that calculated from the simple rule of mixtures. Figure 3 shows that this is not warranted. The increase in the apparent density of the blends from 1.22 g/cm^3 for PVP to 1.45 g/cm^3 for cellulose follows the tie line joining these two densities. This can be rationalized by recalling that only a fraction of the carbonyl groups are interacting with cellulose as shown in the FTIR spectra (Figure 2). Presumably, the interaction of a larger fraction of the different functionalities is necessary to cause a positive deviation from the tie line joining the densities

Table II
Peak Positions in X-ray Diffractograms and ^{13}C Chemical Shifts of Cellulose Polymorphs

polymorph	diffraction angle 2θ, deg						^{13}C chem shifts, ppm			
							C_1	C_4	C_6	C_7[c]
CELL–DMSO[a]	6.3	20.3	21.8	23.3	27.0	35.4	103.3	82.3	63.1	88.9
cellulose I[b]		14.8	16.3	22.6			105.3–106.0	89.1–89.8	63.5–66.2	
cellulose II[b]		12.1	19.8	22.0			105.8–106.3	88.7–88.8	63.5–64.1	
cellulose III_1[b]		11.7	20.7				106.7–106.8	88.0	62.1–62.8	
cellulose IV_1[b]		15.6	22.2				105.6	83.6–84.4	63.3–63.8	
amorphous[b]							ca. 105	ca. 84	ca. 63	

[a] The NMR spectrum of cellulose–DMSO is shown in Figure 11. [b] From ref 23. [c] C_7 is the methylol adduct.

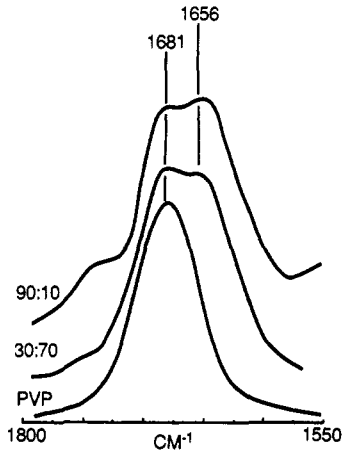

Figure 2. Infrared spectra of PVP and cellulose/PVP 30:70 and 90:10 blends in the carbonyl stretching frequency region.

Table III
Carbonyl Band Absorption Frequency for PVP Blended with Cellulose and Dissolved in Analogue Solvents

	freq, cm^{-1}	shift, cm^{-1}
pure PVP	1681	
PVP dissolved in		
methanol	1664	17
1,4-butanediol	1664	17
cyclohexanol	1669	12
poly(ethylene glycol)-400	1676	5
cellulose/PVP blends	1656	25

of the respective polymers.

Thermal Analysis. Differential scanning calorimetry (DSC) was used to assess the extent of blending between cellulose and PVP. Generally, the observation of a single glass transition temperature (T_g) for a blend pair, between those of the homopolymers, is regarded as decisive evidence of a unique environment and of polymer miscibility, although different methods of measuring T_g are sensitive to different scales of homogeneity.[27] In the present DSC study, however, a single T_g is not necessarily a sign of miscibility, since cast cellulose itself does not show any features to which the glass transition temperature can be related (Figure 4, uppermost curve). On the other hand, the DSC run of PVP (Figure 4, lowest curve) shows a change of slope in the range 150–180 °C, and from the midpoint of the discontinuity of heat flow the T_g was estimated to be 168 °C. For blends with an increasing amount of cellulose, the T_g gradually loses its prominence and becomes more diffuse. Consequently, it becomes increasingly difficult to determine exactly the location of the discontinuity in heat flow as the cellulose content in the blends increases, and it is impossible to locate it in the blends with more than 70% cellulose. Notwithstanding, a gradual increase in the recorded T_g is readily discernible as the composition goes from pure PVP to the 70:30 blend. This demonstrates that, in the blends where the T_g is

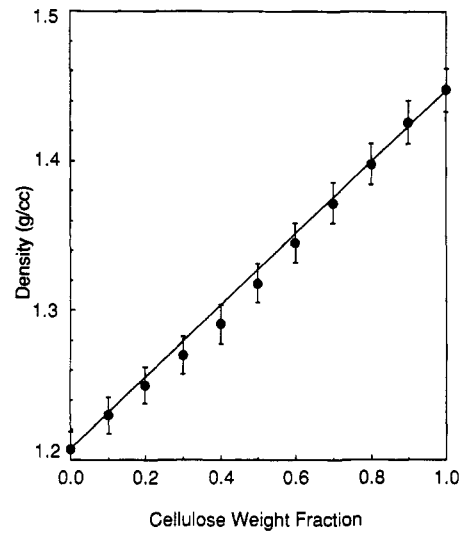

Figure 3. Apparent density of cellulose, PVP, and their blends. All densities are the averages of three measurements. The deviation from the mean is about 1% as shown by the error bars.

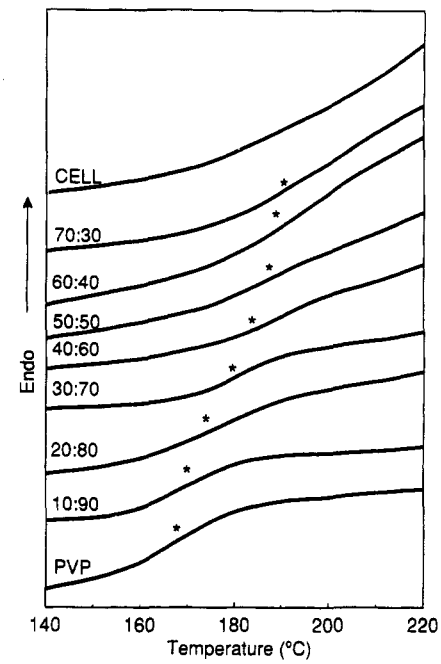

Figure 4. DSC thermograms of cellulose, PVP, and cellulose/PVP blends. The numbers accompanying each curve denote weight percentage of each component. The asterisk marks the position of T_g.

observed, the amorphous phases of the respective polymers are mixing.

Dynamic Mechanical Characterization. In many blend miscibility studies[3-5,27,28] dynamic mechanical analysis (DMA) has proven to be more sensitive than calori-

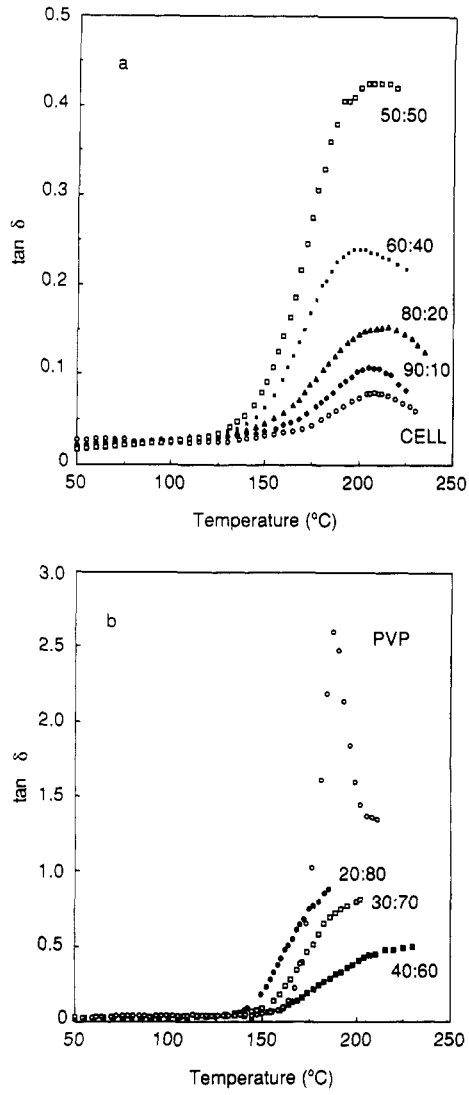

Figure 5. Temperature dependence of tan δ for cellulose, PVP, and their blends. The numbers accompanying each curve denote weight percentage of each component.

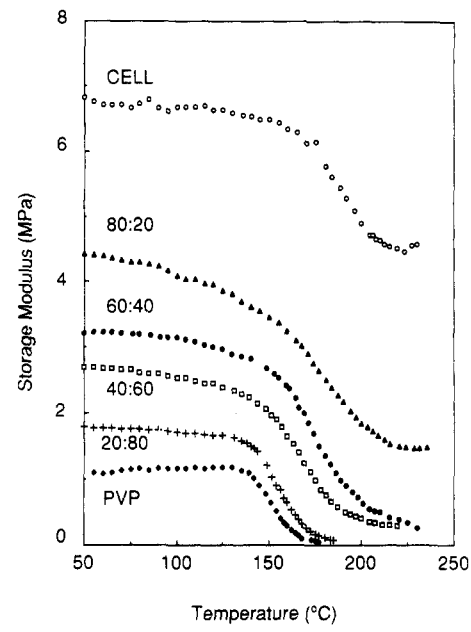

Figure 6. Temperature dependence of the storage modulus (E') for cellulose, PVP, and their blends.

metric measurements for the detection of T_g. Accordingly, we measured the dynamic mechanical relaxation spectra of the blends, hoping to find the transition of the blends with more than 70% cellulose. The results are given in Figure 5–7.

The cast cellulose specimen shows a transition at 208 °C (Figure 5a). Because previous cellulose blend studies[3-5] did not reveal any clearly discernible transition in cellulose below 220 °C, this seemed rather surprising. The transition is possibly the T_g of cellulose lowered, from the estimated T_g of 250 °C for unmodified cellulose,[3,29] by the presence of the residual methylol substituents and/or the presence of plasticizing DMSO. This is consistent with the fact that the T_g of cellulose is depressed by substituents[29] and DMSO is known to interact with oligosaccharides.[30]

As mentioned before, the sensitivity of DMA is greater than that of DSC. However, despite this higher sensitivity the transition monitored at 208 °C is still very weak considering the scale to which it is shown in Figure 5a. It is thus not surprising that the transition was imperceptible by DSC.

The DMA spectra of PVP and the blends are shown in Figure 5. With the exception of PVP, all the measurements were performed with the Rheovibron viscoelastometer (see Experimental Section) on cast films that had a thickness of ca. 50 μm. PVP was run on a dynamic mechanical thermal analyzer (DMTA) using a much thicker 2000-μm melt-pressed sample. This was necessary because we could not measure the tan δ peak of PVP cast films with the Rheovibron due to the excessive softness of PVP at temperatures approaching 180 °C, conjugated with the fact that at this temperature than tan δ values transcended the range covered by the Rheovibron. The tan δ vs temperature plot of PVP shows a single transition centered at 187 °C, which is close to the glass transition of high molecular weight PVP obtained by calorimetry.[31] The high amplitude of this transition reflects well the high mobility of the amorphous polymer at the glass transition, in contrast with cellulose, which shows a weak transition due to its rigid anhydroglucose units.

As cellulose is blended with PVP, the decrease in the temperature of the onset of the transition particular to every blend is conspicuous (Figure 5a). In addition, a broadening of the transition as well as an increase in its magnitude is apparent, although for blends with more than 50% PVP it was not possible to measure the maximum in the tan δ peak, as was the case for pure PVP as explained previously. It is thought that the increase in the breadth of the tan δ peak is not due to incomplete mixing of the two polymers but is rather a consequence of the close proximately of the T_gs of the homopolymers, namely 187 and 208 °C for PVP and cellulose, respectively.

Like the temperature dependence of tan δ, the storage modulus (E') displays a single transition for PVP (Figure 6). The initial (or frozen) values of E' for cellulose and PVP also reflect the relative stiffness of the former in comparison with the latter as a factor of ca. 6 differentiates the moduli. As the cellulose content in the blend increases the initial modulus increases monotonically; furthermore, the midpoint of the plunge in the E' vs temperature curves appears systematically, as every sample goes through its glass transition, at a higher temperature, increasing from ca. 150 °C for PVP to ca. 195 °C for cellulose. Never is there a plateau or a break in the decreasing portion of the curves that would reveal the presence of phase separation.

Figure 7 shows the temperature dependence of the loss modulus (E''). PVP (Figure 7a) displays a T_g peak at 148 °C, and cellulose a T_g peak at 208 °C (Figure 7b). This

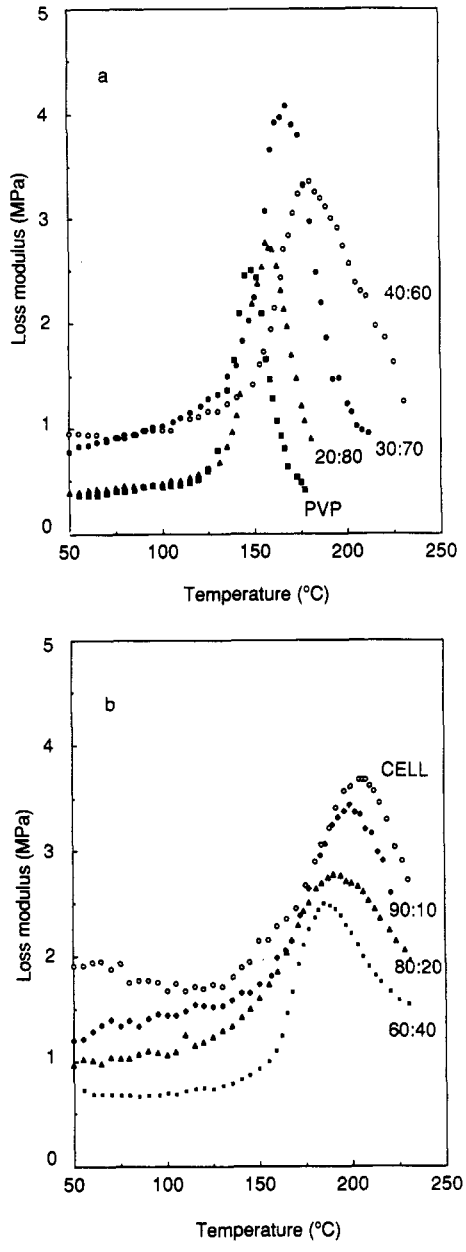

Figure 7. Temperature dependence of the loss modulus (E'') for cellulose, PVP, and their blends.

difference of 60 °C between the loss modulus peaks of the homopolymers allows a complete and precise assessment of the location of the T_g of the blends. This was not possible from DSC measurements and difficult from the storage modulus curves. The loss modulus curves show that the T_g increases as the composition of the blends varies from pure PVP to pure cellulose. This behavior is consistent with the observed trend of the DSC results. In addition, the overall magnitude of the peaks remains practically constant over the whole composition range, and broadening of these transition peaks, which would indicate incomplete mixing of the polymers, is absent. The precise locations of the loss modulus peaks are shown in Table IV along with the values of T_g obtained by DSC. It may be noted that the T_g values obtained by the two techniques are not identical. This should not be surprising because the different methods used for measuring T_g are sensitive to various molecular processes[28] that may not occur at the same temperature.

T_g–Composition Relationship. There are several classical equations that correlate the glass transition temperature of a miscible blend system with its composition. The simplest of these relations is the rule of mixtures:

Table IV
T_g As Obtained from DSC and DMA for Cellulose, PVP, and Their Blends

blend comp[a]	temp, °C DSC	temp, °C DMA[b]
0/100	168	148
10/90	170	153
20/80	174	158
30/70	179	165
40/60	184	168
50/50	187	172
60/40	188	174
70/30	190	178
80/20	ND[c]	190
90/10	ND	199
100/0	ND	208

[a] CELL/PVP (w/w). [b] E'' peak. [c] ND: not determined.

$$T_g = W_1T_{g1} + W_2T_{g2} \quad (1)$$

where T_g, T_{g1}, and T_{g2}, are the glass transition temperatures of the blend, homopolymer 1, and homopolymer 2, respectively. W_1 and W_2 are the corresponding weight fractions. With the same parameters it is possible to write the Fox equation[32] as

$$1/T_g = W_1/T_{g1} + W_2/T_{g2} \quad (2)$$

In the Gordon and Taylor equation[33] an additional parameter is introduced:

$$T_g = (W_1T_{g1} + kW_2T_{g2})/(W_1 + kW_2) \quad (3)$$

where k is the ratio of the volume expansion coefficients of the homopolymers in the mixture. Similarly, the Jenckel and Heusch equation[34] has an empirical parameter, b, which varies from system to system:

$$T_g = W_1T_{g1} + W_2T_{g2} + W_1W_2b(T_{g1} - T_{g2}) \quad (4)$$

Finally, Kwei proposed[35] an equation in which an interaction term q is introduced:

$$T_g = (W_1T_{g1} + kW_2T_{g2})/(W_1 + kW_2) + qW_1W_2 \quad (5)$$

These equations have been used to interpret both positive[36] and negative[37] deviations from the rule of mixtures, as well as S-shaped[35,38] T_g vs composition curves.

With the E'' data obtained over the whole composition range, we calculted the T_gs predicted by these semiempirical relationships. The result of the curve-fitting procedures is shown in Figure 8. For the cellulose/PVP pair, where the difference in T_g between the two polymers, given by their respective E'' values, is 60 °C, the predictions of the different models are very close to one another. Furthermore, each model predicts a regular monotonic increase in the T_g. In contrast, as seen in Figure 9, the experimentally observed spectrum shows two regions with a striking discontinuity at a blend composition corresponding to about 60% (w/w) cellulose. It is interesting to note that Kovacs developed a free volume theory[39,40] that predicts a discontinuity at a critical temperature T_c, where $T_c = (T_{g2} - 52), T_{g2} > T_{g1}$.[41] However, as was shown by Aubin and Prud'homme,[41] this discontinuity is hardly noticeable for polymers that differ by less than ca. 75 °C in their respective T_g, as is the case for the present polymer pair. In addition, Kovacs' theory predicts that below T_c the plot is concave upward, which is not consistent with the behavior displayed in Figure 9 below the discontinuity.

The unusual trend exhibited by the T_g vs composition curve of the cellulose/PVP blends can be given a plausible

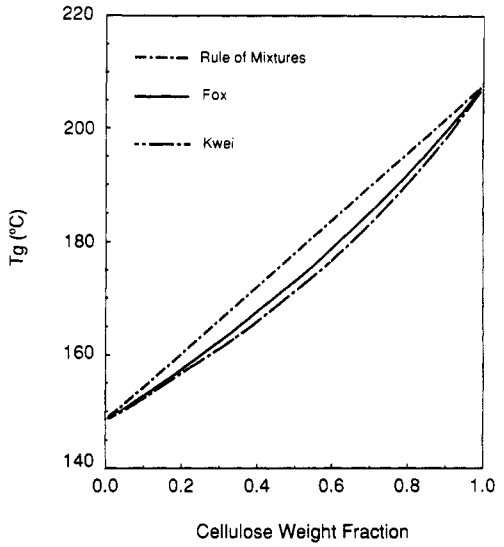

Figure 8. Theoretical glass transition temperatures of cellulose/PVP blends as a function of weight fraction according to the equations proposed by Fox (eq 2) and Kwei (eq 5). The curves calculated with the equations proposed by Gordon and Taylor (eq 3) and Jenckel and Heusch (eq 4) overlap with those of Fox and Kwei and were omitted for clarity of presentation; the straight line is the expected glass transition temperature from the rule of mixtures.

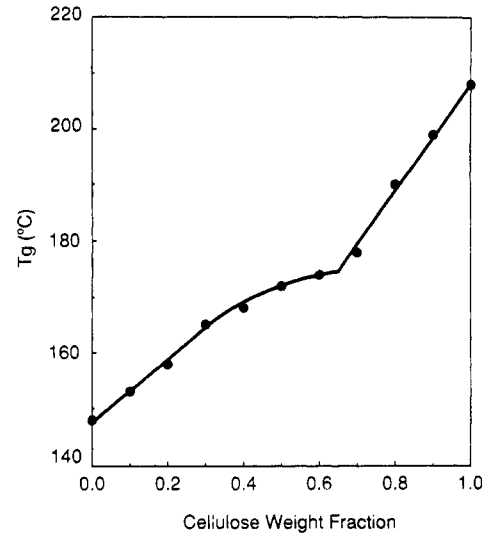

Figure 9. Glass transition temperature of cellulose/PVP blends as a function of cellulose weight fraction as obtained from dynamic mechanical loss moduli.

explanation if the molar ratio of the repeating unit of the respective polymers for different compositions is taken into account. Figure 10 shows the molar ratio of the repeating unit of cellulose (anhydroglucose, AHG) to PVP, the molar ratio of hydroxyl groups to PVP repeating units, and their reciprocal ratios as a function of blend composition. Of particular importance are the points designated by A and B. At point A, which corresponds roughly to a blend composition of 60:40, cellulose and PVP are present in equimolar quantities in terms of their respective repeating units. In other words, when the AHG/PVP molar ratio is equal to one, for each AHG unit of cellulose one carbonyl group of PVP is present in the mixture. Thus, in the composition range 0–60% (w/w) cellulose in the blend, where the AHG/PVP molar ratio is less than one, there are always more carbonyl groups in the mixture than there are AHG units to which they can bind. Consequently, below 60% (w/w) cellulose in the blend, only a portion of the carbonyl groups of PVP can interact with

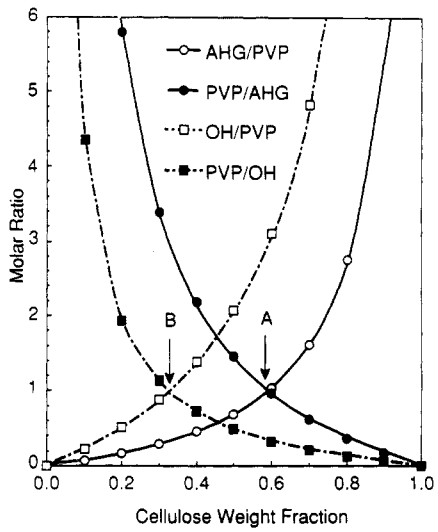

Figure 10. Molar ratio of the repeating anhydroglucose unit of cellulose (AHG) to PVP, molar ratio of hydroxyl groups (OH) to PVP, and their reciprocal ratios as a function of the cellulose weight fraction in the blend. The molar ratios were calculated from the relative content of cellulose and PVP in the blends. The points correspond to the cellulose weight fractions for which the molar ratios were calculated.

cellulose. This is in accordance with the presence of two carbonyl peaks in the IR spectra of the blends, one for the carbonyls that are not interacting with cellulose and another for those that are hydrogen bonded. It is interesting to note that in Figure 9 the curvature between 40% and 60% (w/w) cellulose in the blends lies in the region between points A and B in Figure 10. At point B, just above 30% (w/w) cellulose in the blend, there is a one-to-one correspondence in the number of carbonyl and hydroxyl groups in the mixture so that between 40% and 60% (w/w) cellulose in the blend we go from a one-to-one correspondence between the number of interacting groups of cellulose and PVP to a one-to-one correspondence between the number of AHG units and PVP units (where there is a 3:1 hydroxyl to carbonyl ratio). Thus for the blends with 40, 50, and 60% (w/w) cellulose there are enough hydroxyl groups in the mixtures for all the carbonyl groups to interact. However, we already know from the FTIR measurements that only a portion of the carbonyl groups are interacting; consequently, for those carbonyl groups that do interact with cellulose, it is possible that they interact simultaneously with more than one hydroxyl group. Evidence of this behavior is also provided by the FTIR results as discussed earlier. Further discussion of the T_g–composition curve will be presented later.

CP-MAS NMR. The solid-state ^{13}C spectra for PVP, cellulose, and three blends are displayed in Figure 11. The carbon resonance peaks of PVP were assigned to specific ring and backbone carbons with the aid of the published ^{13}C solution spectra of PVP.[42,43] The carbonyl carbon appears at 175 ppm, well separated from the peaks at 42, 33, and 20 ppm that correspond to the overlapping of the ring and main-chain carbon resonances. For cellulose, the carbon resonances were readily correlated to specific anhydroglucose carbons with tables of the chemical shifts for cellulose polymorphs.[23,44] The resonance peak at 88.9 ppm was assigned to the methylol adduct after comparison with the spectrum of resole.[45] The peak at 40 ppm arises from the DMSO bound to the anhydroglucose units. The chemical shifts for the C_1, C_4, C_6, and C_7 (methylol adduct) carbons of cellulose are given in Table II. The difference between the chemical shifts of these carbons

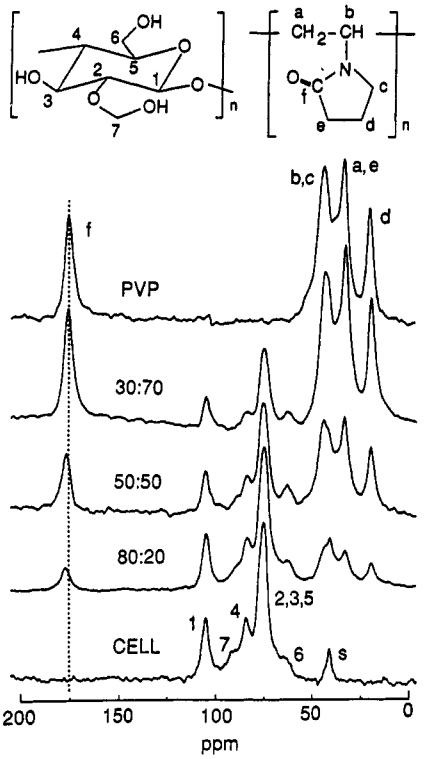

Figure 11. CP-MAS spectra of PVP, cellulose, and three blends. The labeled peaks correspond to the carbons identified in the chemical structure. The peak identified as S in the cellulose spectrum corresponds to bound DMSO. Note that the methylol adduct (C_7OH) can also be on O_2H or O_3H.

and those of the cellulose I–IV polymorphs supports the existence of a different crystal lattice in the crystalline regions of cast cellulose as suggested by its X-ray diffractogram.

The spectra of the blends exhibit three outstanding features. First, the carbonyl peak of PVP appears at a lower field in the blends than in the pure homopolymer. This is consistent with the observed shift of the infrared frequency of the carbonyl group. Second, the methylol resonance (C_7), appearing as a shoulder in the spectrum of cellulose, almost vanishes in the blends. This is most apparent in the 30:70 blend. Third, the C_6 peak of cellulose is distinct in the blends while in contrast it appears as a shoulder in unblended cellulose. Since changes in chemical shifts or line shapes of the blend components relative to their respective homopolymers are observed, cellulose and PVP must mix on an individual chain to chain basis. Because the changes in line shapes and shifts are observed mostly at the carbonyl carbon of PVP and at the peaks of the C_6 and C_7 pendant carbons of the anhydroglucose unit of cellulose, it is reasonable to assume that the interaction between the two polymers is directed through the functionalities attached at these carbons, namely the oxygen of the carbonyl groups of PVP, the primary hydroxyl groups of the unsubstituted C_6, and the methylol adduct of cellulose, whether it be on C_2, C_3, or C_6.

$T_{1\rho}$ Measurements. When the state of miscibility of a blend is discussed, the scale of the mixing has to be taken into consideration. A particular blend may be characterized as miscible with one technique and immiscible with another.[27] The limit of resolution inherent to the technique used to characterize the blend system permits the estimation of the upper limit of the scale of miscibility. For example, visual determination of optical clarity establishes the absence of heterogeneities exceeding ca. 500 nm in size. The T_g measured by DSC is sensitive

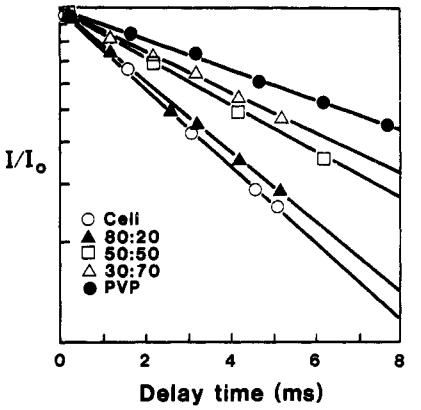

Figure 12. Semilogarithmic plot of the measured relative ^{13}C CP/MAS resonance intensity versus delay time for cellulose, PVP, and three cellulose/PVP blends. The slope yields the proton relaxation time, $T_{1\rho}$.

Table V
Proton $T_{1\rho}$ for Solid Films of Cellulose and PVP in Their Blended and Unblended States

	$T_{1\rho}$,[a] ms	
cellulose/PVP blend	cellulose	PVP
0/100		10.8
30/70	7.3	7.3
50/50	6.2	6.3
80/20	4.2	4.2
100/0	4.2	

[a] ±5%.

to heterogeneities with sizes of ca. 25–30 nm, while the dynamic mechanical analysis is more sensitive with an upper limit of 15 nm.[46] From spin-diffusion measurements it is possible to estimate the size of heterogeneities in the range of a few angstroms to a few tens of nanometers.[11-13]

When the scale of phase separation in the blend is sufficiently small to permit rapid spin diffusion and cause the observed magnetization intensity to decay as a single-exponential function after it has been disturbed, then it is possible to estimate the upper limit of domain size from the equation[11]

$$L^2 \approx (t/T_2)d^2 \tag{6}$$

where L^2 is the mean-square distance over which diffusion is effective, d is the distance between protons, t is the measured relaxation time, in this instance $T_{1\rho}$, and T_2 is the spin–spin lattice relaxation time. Typically, d is ca.0.1 nm and below the glass transition T_2 is ca. 10 μs. Thus in this present case the above equation can be reduced to

$$L \approx (T_{1\rho})^{1/2} \tag{7}$$

with L in nanometers and $T_{1\rho}$ in milliseconds.

The relaxation times $T_{1\rho}$ for cellulose, PVP, and the 30:70, 50:50, and 80:20 blends were obtained from the slope of a semilogarithmic plot of the intensity vs the delay time used in a delayed cross-polarization experiment[16,47] (Figure 12). All the blends showed a single-exponential decay, revealing the absence of heterogeneities of the scale covered by spin diffusion. The relaxation times were identical for all peaks of the spectrum, indicating efficient proton spin coupling in the blends. The results of the $T_{1\rho}$ experiments on the different samples are shown in Table V. The relaxation times for PVP and cellulose are 10.8 and 4.2 ms in their respective unblended states. In the 30:70 and 50:50 blend the $T_{1\rho}$ values of both components are practically identical while being different from the values of the homopolymers. This reveals thorough mixing on a scale that is readily calculated to be ca. 2.7 nm with eq

7. However, because of uncertainty as to the exact value of d and T_2 in eq 6, this estimate of the scale of mixing is subject to an error limit of about 50%. On the other hand, although the $T_{1\rho}$ values of both components are the same in the 80:20 blend, this value is identical to that of unblended cellulose. This irregularity can be explained in at least three different ways, not all of which stand up to close scrutiny. First, identical $T_{1\rho}$ values for cellulose in the 80:20 blend and in the unblended state could indicate that $T_{1\rho}$ is determined by the residual crystallinity of cellulose in these specimens; i.e., the lower relaxation rate of the crystalline phase in comparison to the amorphous phase is rate determining. This possibility, however, must be discarded because WAXS has shown that the crystallinity of cellulose decreases as it is blended with PVP. A reduction in crystallinity would necessarily cause a change in the measured $T_{1\rho}$ of cellulose in the blend, which is not the case. The second possibility is that the rates of relaxation of cellulose in the 80:20 blend and in the unblended state lie close together on the broad minimum of the U-shaped $T_{1\rho}$ vs rate of motion (correlation time, τ_c) curve so that the measured $T_{1\rho}$ values are identical (see ref 11 for an in-depth presentation of the interrelation between the relaxation and correlation times). This possibility can also be ruled out because in another 80:20 cellulose blend[48] the $T_{1\rho}$ of cellulose is not identical to that of unblended cellulose, from which it follows that the $T_{1\rho}$ of cellulose in the present 80:20 blend does not lie at the minimum of the $T_{1\rho}$ vs τ_c curve. The third and most plausible possibility is that cellulose acts as a matrix in which PVP is imbedded, so that the 80:20 blend would be inhomogeneous on a molecular scale. In such a matrix, the motions of cellulose in the blend would remain undisturbed and the relaxation rate would also remain constant. The rationale for considering the 80:20 blend as one where cellulose is a matrix hosting PVP can be understood by examining Figure 10. Above 60% cellulose in the blend less than one carbonyl per AHG unit is present in every blend. It is thus possibly increasingly difficult for cellulose to blend extensively with the PVP as the number of carbonyl groups decreases. The same argument could be used to justify incomplete blending below 60% cellulose; however, the number of hydroxyl groups is 3 times that of the number of AHG units, so that below 60% cellulose in the blend there are always sufficient hydroxyl groups in the mixture for cellulose and PVP to mix on a segmental level as calculated above.

In light of these results it is now possible to correlate the T_g vs composition curve to the extent of mixing of the different blends. Below 60% cellulose in the blend, cellulose and PVP mix on a segmental scale with an upper limit of ca. 2.7 nm. The curvature between 40% and 60% cellulose arises from what can be termed "saturation", where for every carbonyl unit there is between one and three hydroxyl groups with which it can interact. Above 60% cellulose in the blend, cellulose and PVP mix on a scale between ca. 2.7 and ca. 15 nm. This is a consequence of the fact that the $T_{1\rho}$ value of cellulose in the 80:20 blend and in its unblended state is identical, revealing little blending of cellulose on a 2.7-nm scale and that for every blend a single T_g is observed by DMA, which reveals an upper limit in heterogeneity on a scale of 15 nm. Thus although for all blend compositions a single T_g is observed, so that cellulose and PVP can be characterized as fully miscible, the discontinuity in the T_g vs composition curve corresponds to the point where the level of miscibility between the two polymers changes.

Concluding Remarks

The results reported in this paper provide a clear indication that blends of cellulose with PVP are miscible over the whole composition range and that the miscibility is driven by hydrogen bond formation between the hydroxyl groups of cellulose and carbonyl functionalities of PVP. The plot of the measured T_g vs composition is not a smooth function but shows a singularity at a blend composition of ca. 60:40 cellulose/PVP (w/w). This is perhaps the most significant result of the present study. When this behavior is analyzed in terms of the molar ratio of the repeating units of the component polymers, it is seen that the singularity corresponds to the composition where the molar ratio is unity. This result has been tentatively interpreted in terms of solid-state NMR data. $T_{1\rho}$ measurements on the two components in the blends suggest that below the discontinuity in the T_g–composition curve the two polymers mix on a segmental scale (2.7 nm) whereas they mix on a somewhat larger scale above the discontinuity. The scale of miscibility has been correlated with the relative abundance of carbonyl and hydroxyl groups available for molecular interaction. It is thought that below the discontinuity enough hydroxyl groups are present in the blends to interact with all of the carbonyls of PVP and produce mixing on a segmental level, whereas above the discontinuity the number of carbonyls in the blends is too low to achieve miscibility on the same scale.

A change of miscibility across the composition spectrum is not a novelty since some polymer pairs are known to be miscible at one composition and immiscible at another.[49,50] However, for two polymers that are miscible over the whole composition range, a change in the scale of miscibility that manifests itself as a discontinuity in the T_g–composition curve has not previously been observed, as far as we know.

Since it is thought that the scale of mixing is closely related to the molar ratio of the interacting groups in the blends and since the miscibility is driven by the interaction of only a portion of the carbonyl groups of PVP or of the hydroxyl groups of cellulose, as has been shown by FTIR and CP-MAS NMR, a reduction in the total number of available groups in either one or even both polymers would still possibly lead to miscibility. This raises the question as to the minimum number of interacting groups necessary for the two polymers to remain miscible. It has already been demonstrated[51,52] that the number of favorable interactions necessary to drive blend miscibility is surprisingly low in some cases. For example, a number of immiscible polystyrene/polyacrylate blend pairs were rendered miscible by the introduction of as little as 1–2% vinylphenol in polystyrene.[51] Cellulose/synthetic polymer blends lend themselves to this kind of inquiry since systematic changes in chemical structure can readily be made by altering the degree of substitution of the cellulose component. This would be an interesting avenue for further experiments.

Acknowledgment. J-F.M. thanks Dr. Y. Nishio (Nagaoka University of Technology) for helpful comments and suggestions, Dr. L. A. Belfiore (Colorado State University) for stimulating and helpful discussions, and Dr. F. Morin (McGill University) for his assistance in performing the NMR experiments. The financial support of the Natural Sciences and Engineering Research Council of Canada, the Fonds pour la Formation de Chercheurs et l'Aide à la Recherche, and the Pulp and Paper Institute of Canada is also acknowledged.

References and Notes

(1) *Polymer Blends*; Paul, D. R., Newman, S., Eds.; Academic: New York, 1978.
(2) Olabisi, O.; Robeson, L. M.; Shaw, M. T. *Polymer–Polymer Miscibility*; Academic: New York, 1979.
(3) Nishio, Y.; Roy, S. K.; Manley, R. St. J. *Polymer* **1987**, *28*, 1385.
(4) Nishio, Y.; Manley, R. St. J. *Macromolecules* **1988**, *21*, 1270.
(5) Nishio, Y.; Manley, R. St. J. *Polym. Sci. Eng.* **1990**, *30*, 71.
(6) Nishio, Y.; Hirose, N.; Takahashi, T. *Polym. J.* **1989**, *21*, 347.
(7) Jolan, A. H.; Prud'homme, R. E. *J. Appl. Polym. Sci.* **1978**, *22*, 2533.
(8) Seymour, R. B.; Johnson, E. L.; Stahl, G. A. *Macromolecular Solutions*; Seymour, R. B., Stahl, G. A., Eds.; Pergamon Press: New York, 1982; pp 90–100.
(9) Field, N. D.; Song, S. S. *J. Polym. Sci., Polym. Phys. Ed.* **1984**, *22*, 101.
(10) *Polymer Blends and Mixtures*; Walsh, D. J., Higgins, J. S. Maconnachie, A., Eds.; NATO Advanced Study Institute Series E, No. 89; Martinus Nijhoff Publishers: Dordrecht, 1985.
(11) McBrierty, V. J.; Douglass, D. C. *J. Polym. Sci., Macromol. Rev.* **1981**, *16*, 295.
(12) Linder, M.; Hendrichs, P. M.; Hewitt, J. M.; Massa, P. J. *J. Chem. Phys.* **1985**, *82*, 1585.
(13) Parmer, J. F.; Dickenson, L. C.; Chien, J. C. W.; Porter, R. S. *Macromolecules* **1989**, *22*, 1078.
(14) Seymour, R. B.; Johnson, E. L. *J. Appl. Polym. Sci.* **1976**, *20*, 3425.
(15) Walker, J. F. *Formaldehyde*, 2nd ed.; ACS Monogr. Ser. 159; Reinhold: New York, 1953; p 382.
(16) Stejskal, E. O.; Schaefer, J.; Sefcik, M. D.; McKay, R. A. *Macromolecules* **1981**, *14*, 275.
(17) Johnson, D. C.; Nicholson, M. D.; Haig, F. C. *Appl. Polym. Symp.* **1976**, *28*, 931.
(18) Swenson, H. A. *Appl. Polym. Symp.* **1976**, *28*, 945.
(19) Baker, T. J.; Schroeder, L. R.; Johnson, R. B. *Carbohydr. Res.* **1978**, *67*, C4.
(20) Baker, T. J.; Schroeder, L. R.; Johnson, R. B. *Cellulose Chem. Technol.* **1981**, *15*, 311.
(21) Shiraishi, N.; Katayama, T.; Yokota, T. *Cellulose Chem. Technol.* **1978**, *12*, 429.
(22) Patton, P. A.; Gilbert, R. D. *J. Polym. Sci., Polym. Phys. Ed.* **1983**, *21*, 515.
(23) Isogai, A.; Usuda, M.; Kato, T.; Uryu, T.; Atalla, R. H. *Macromolecules* **1989**, *22*, 3168.
(24) Nishio, Y.; Haratani, T.; Takahashi, T. *J. Polym. Sci., Part B* **1990**, *28*, 355.
(25) Coleman, M. M.; Painter, P. C. *Appl. Spectrosc. Rev.* **1984**, *20*, 255.
(26) Moskala, E. J.; Varnell, D. F.; Coleman, M. M. *Polymer* **1985**, *26*, 228.
(27) Stoelting, J.; Karasz, F. E.; MacKnight, W. J. *Polym. Eng. Sci.* **1970**, *10*, 133.
(28) McKnight, W. J.; Karasz, F. E.; Fried, J. R. Reference 1, Chapter 5.
(29) Kamide, K.; Saito, M. *Polym. J.* **1985**, *17*, 919.
(30) Cacu, B.; Reggiani, M.; Gallo, G.; Vigevani, A. *Tetrahedron* **1966**, *22*, 3061.
(31) Turner, D. T.; Schwartz, A. *Polymer* **1985**, *26*, 757.
(32) Fox, T. G. *Bull. Am. Phys. Soc.* **1956**, *1*, 123.
(33) Gordon, M.; Taylor, J. S. *J. Appl. Chem.* **1952**, *2*, 495.
(34) Jenckel, F.; Heusch, R. *Kolloid Z.* **1953**, *30*, 89.
(35) Kwei, T. K. *J. Polym. Sci., Polym. Lett. Ed.* **1984**, *22*, 307.
(36) Rodriguez-Parada, J. M.; Percec, V. *Macromolecules* **1986**, *19*, 55.
(37) Pugh, C.; Percec, V. *Macromolecules* **1986**, *19*, 65.
(38) Pennacchia, J. R.; Pearce, E. M.; Kwei, T. K.; Bulkin, B. J.; Chen, J.-P. *Macromolecules* **1986**, *19*, 973.
(39) Kovacs, A. J. *Adv. Polym. Sci.* **1963**, *3*, 394.
(40) Braun, G.; Kovacs, A. J. *Physics of Non-Crystalline Solids*; Prins, J. A., Ed.; North-Holland: Amsterdam, 1965; p 303.
(41) Aubin, M.; Prud'homme, R. E. *Macromolecules* **1988**, *21*, 2945.
(42) Cheng, H. N.; Smith, T. E.; Vitus, D. M. *J. Polym. Sci., Polym. Lett. Ed.* **1981**, *19*, 29.
(43) Yokota, K.; Abe, A.; Hosaka, S.; Sakai, I.; Saito, H. *Macromolecules* **1978**, *11*, 95.
(44) Fyfe, C. A.; Dudley, R. A.; Stephenson, P. J.; Deslandes, Y.; Hamer, G. K.; Marchessault, R. H. *Rev. Macromol. Chem. Phys.* **1983**, *C23*, 187.
(45) Fyfe, C. A.; Rudin, A.; Tchir, W. J. *Macromolecules* **1980**, *13*, 1322.
(46) Kaplan, D. S. *J. Appl. Polym. Sci.* **1976**, *20*, 2615.
(47) Parmer, J. F.; Dickinson, L. C.; Chien, J. C. W.; Porter, R. S. *Macromolecules* **1989**, *22*, 1078.
(48) Masson, J-F.; Manley, R. St. J. *Macromolecules*, in press.
(49) Nassar, T. F.; Paul, D. R.; Barlow, J. W. *J. Appl. Polym. Sci.* **1979**, *23*, 85.
(50) Cruz, C. A.; Paul, D. R.; Barlow, J. W. *J. Appl. Polym. Sci.* **1980**, *25*, 1549.
(51) Chen, C.-T.; Morawetz, H. *Macromolecules* **1989**, *22*, 159.
(52) Serman, C. J.; Xu, Y.; Painter, P. C.; Coleman, M. M. *Macromolecules* **1989**, *22*, 2015.

Registry No. PVP, 9003-39-8; cellulose, 9004-34-6.